Available online at www.sciencedirect.com
SCIENCE DIRECT®
Icarus 169 (2004) 482–491
ICARUS
www.elsevier.com/locate/icarus

Watching meteors on Triton

W. Dean Pesnell,[a,*] J.M. Grebowsky,[b] and Andrew L. Weisman [c]

[a] *Nomad Research, Inc., 795 Scarborough Court, Arnold, MD 21012-1336, USA*
[b] *Planetary Magnetospheres Branch, Code 695.1, NASA/Goddard Space Flight Center, Greenbelt, MD 20771, USA*
[c] *River Hill High School, 13849 Russell Zep Drive, Clarkesville, MD 21029, USA*

Received 13 June 2003; revised 12 January 2004

Available online 12 April 2004

Abstract

The thin atmosphere of Neptune's moon Triton is dense enough to ablate micrometeoroids as they pass through. A combination of Triton's orbital velocity around Neptune and its orbital velocity around the Sun gives a maximum meteoroid impact velocity of approximately 19 km s^{-1}, sufficient to heat the micrometeoroids to visibility as they enter. The ablation profiles of icy and stony micrometeoroids were calculated, along with the estimated brightness of the meteors. In contrast to the terrestrial case, visible meteors would extend very close to the surface of Triton. In addition, the variation in the meteoroid impact velocity as Triton orbits Neptune produces a large variation in the brightness of meteors with orbital phase, a unique Solar System phenomenon.

Keywords: Meteoroids; Atmosphere, composition; Ionosphere

1. Introduction

The meteoric influx into the terrestrial atmosphere, and its consequences within the atmosphere and ionosphere, has been well studied, with data from satellites, rockets, lidar, and photometric observations (see reviews by Grün et al. (2001), Murad and Williams (2002)). By comparison, relatively few measurements of the micrometeoroid fluxes in the outer Solar System are available (Grün et al., 1985, 2001). There are also possibly important consequences of meteoroid input to the atmospheres of minor bodies in the Solar System. The effects of meteoroid input on planets other than Earth have only deduced from models. Nevertheless, these models indicate that micrometeoroids lead to significant phenomena in all planetary atmospheres. For example, Ip (1990a) and Molina-Cuberos et al. (2001) have highlighted some of the properties of meteoroid impacts with the Titan atmosphere and showed that the meteoric input could produce a significant perturbation in the atmosphere or ionosphere of a minor planet in the Solar System. The effects of meteoroids at Triton, the only other moon in the Solar System with a substantial atmosphere, have not been previously studied and are the subject of this paper.

Triton orbits Neptune in the far reaches of the Solar System. Although micrometeoroids hitting the atmosphere accelerated only by the weak gravity of Triton would not be heated to evaporation, the combination of the micrometeoroid's orbital velocity, Triton's orbital speed, and the gravitational accelerations of Triton and Neptune results in a sufficiently high velocity of impact that some particles are heated to visibility. Triton is in a retrograde orbit about Neptune and in synchronous rotation, with one side continuously facing Neptune. Micrometeoroids will be swept up by the leading face of Triton, which is therefore the location where most meteors would be seen. The Triton–Neptune configuration and Triton's thin, but not insignificant, atmosphere, make a unique environment in the Solar System for studying meteor physics.

Two radio occultation electron density profiles and several theoretical model ionospheres have been published for Triton (Tyler et al., 1989; Lyons et al., 1992; Ip, 1990b). All show a prominent main layer consisting likely of either C^+ or N^+ located above an altitude of 200 km. The ionization is caused by a combination of solar radiation and energetic electron precipitation. Below 200 km, the occultation measurements indicate a possibility of additional, lower altitude,

* Corresponding author. Fax: 301-286-1651.
E-mail address: pesnell@nomadresearch.com (W. Dean Pesnell).

0019-1035/$ – see front matter
doi:10.1016/j.icarus.2004.01.011

ion layers (Lyons et al., 1992). These low-altitude layers could consist of metal atoms and metallic compounds left behind by ablating micrometeoroids that had been photoionized by the solar UV irradiance. Remnants of meteoroids, or the recondensed products of the ablated material, could also serve an important role as nucleation sites of the cloud particles that cause the haze layers observed in Triton's atmosphere (Yelle et al., 1995).

A theoretical investigation of the brightness and frequency of meteors in Triton's atmosphere would illustrate some of the expected consequences of that meteoroid input. With this goal in mind, a study of the meteor production and meteoric input at Triton was done to determine the relative importance of each of the possible meteoric ionization processes and to isolate those processes that require additional research. When further observations are made of the Triton environment, the results of this study will provide a basis for better defining the micrometeoroid distribution in the outer Solar System. In this work we will focus on the visibility of meteors in Triton's atmosphere, because of its unique spatial distribution compared to other Solar System atmospheres. In the process we will infer their potential ionospheric and haze contributions.

2. The atmosphere of Triton

Only a few atmospheric mass density profiles for the N_2-dominated atmosphere of Triton have been published. The density and temperature models of Krasnopolsky and Cruikshank (1995) are used in this meteor ablation study. The altitude dependence of the density, temperature, and pressure of this model agrees with the observations of Broadfoot et al. (1989) and is similar to the model of Strobel and Summers (1995). The mixing ratio of the most important minor species is roughly 10^{-4} (CO, Krasnopolsky and Cruikshank, 1995; CH_4, Strobel and Summers, 1995). At such small concentrations the minor species do not play an important role in meteor ablation, which depends only on the column mass density of the atmosphere. The model in Fig. 2 of Krasnopolsky and Cruikshank (1995) was digitized to provide a computer-accessible profile of temperature, pressure, and mass density as a function of altitude (Fig. 1).

The likely existence of meteors in Triton's atmosphere can be demonstrated by comparing the properties of Triton's atmosphere with other, meteor-producing, planetary atmospheres. The local atmospheric column mass density best parameterizes the rate of meteoroid ablation (Bronshten, 1983, Section 3) in that meteors occur at similar column densities in any atmosphere. However, pressure is a more accessible atmospheric parameter. These two quantities are closely related as shown in Fig. 2, which depicts the column mass density as a function of pressure for several planets and Triton.

Terrestrial meteors are formed at an altitude of roughly 90 km, corresponding to a pressure of 2 μbar. This corresponds to an estimated altitude of 30 km in Triton's atmosphere. Two effects will shift the actual meteoroid ablation altitude at Triton away from the terrestrially inferred location. Due to the lower impact speeds at Triton (see below), a meteoroid of a given mass will penetrate to a higher pressure in Triton's atmosphere than the Earth's. Also, because of Triton's lower gravity compared to those of the planets, a given column mass density is intercepted by a meteoroid at a lower pressure on Triton than in other atmospheres, as

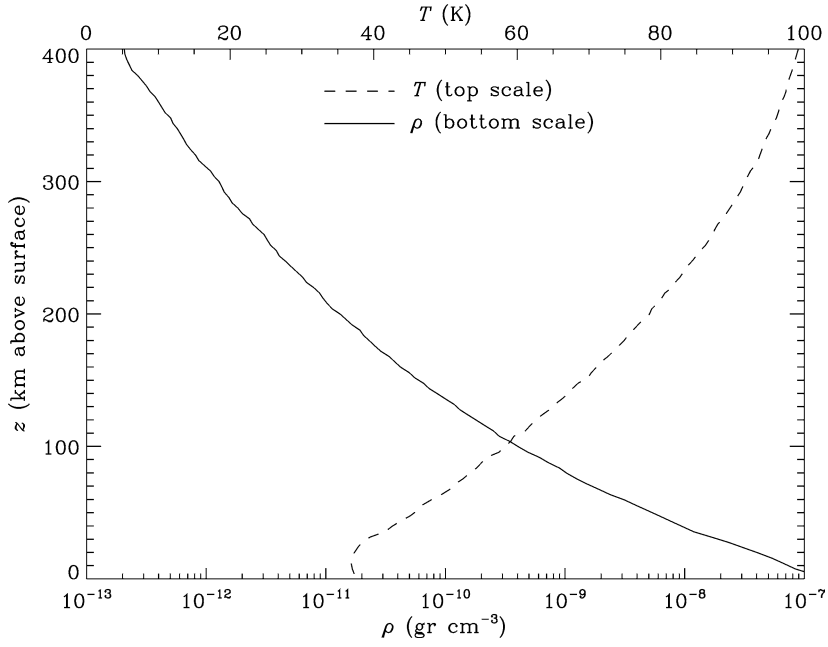

Fig. 1. The variation of mass density (ρ, bottom scale) and temperature (T, top scale) in Triton's atmosphere from Fig. 2 of Krasnopolsky and Cruikshank (1995). Below the lowest altitude resolved by the digitization process the temperature is assumed constant and the density varies exponentially with altitude.

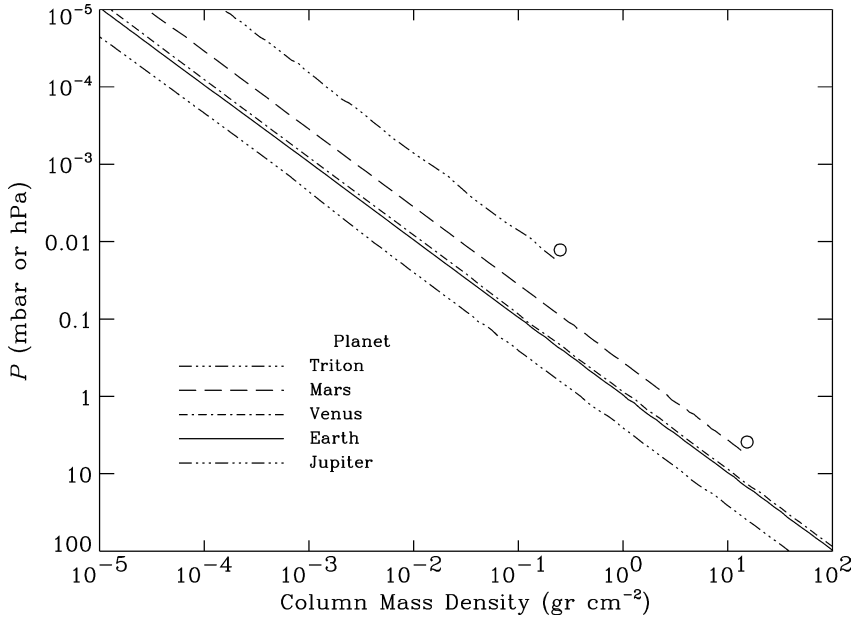

Fig. 2. A comparison of column mass in several atmospheres. The ◯ symbol indicates a surface. Triton's atmosphere is described in Fig. 1 above; the martian atmosphere is discussed in Pesnell and Grebowsky (2000); the cytherean model was computed using the VTS3 model described in Hedin (1983); the terrestrial model is the MSIS model (Hedin, 1987) evaluated at mid-latitudes for moderate solar activity; the jovian model is from Kim et al. (2001).

can be seen in Fig. 2. The known Triton surface pressure of ~ 10 μbar and the observed ablation of meteoroids at a pressure $10\times$ smaller in the terrestrial atmosphere offers strong evidence for the presence of meteors at Triton.

To characterize the meteor intensity at Triton relative to Earth we will refer it to a hypothetical sensor on the surface of Triton. The altitude of ablation determines the effective viewing area of a meteor detector provided by such an instrument. Assuming the opening angle of the detector is 45° and the ablation altitude is 30 km, meteors over an area of 3×10^3 km^2 could be seen by the detector. A more interesting aspect of meteors at Triton is their closeness to the surface. As will be shown, meteoroids could create observable meteors almost to the surface. In contrast, the brightness of terrestrial meteors measured from the ground are usually normalized to an altitude of 100 km (Öpik, 1958).

3. Micrometeoroid environment at Triton

Comets and massive asteroids have bombarded the Earth and other planets since the beginning of the Solar System. In today's Solar System, impacts of large, crater-producing or atmosphere disrupting bodies are rare events that have only an ephemeral effect on a planetary atmosphere and ionosphere during their initial passage. On the other hand, smaller interplanetary particles continuously pelt the planets, providing a persistent source of dust and metallic atoms in all planetary atmospheres. Using Triton's surface as an observation post to study the flux of micrometeoroids in the outer Solar System would provide higher meteor count rates than on spacecraft due to the large field of view of the impact zone and ability to continuously integrate a known volume of space. The composition and velocity distribution of the impacting particles can be deduced from these observations, which would provide valuable information on the Kuiper and Oort clouds.

Interplanetary particle mass flux distributions at Neptune, derived by Moses (1992) from the measured interplanetary distribution of Grün et al. (1985), were used to estimate the occurrence rate of visible meteors in Triton's atmosphere. Moses (1992) assumed two velocity populations of micrometeoroids: Oort cloud particles, whose orbits have high eccentricities and random inclinations; and Neptune family particles, with more circular, prograde, low-inclination orbits. The impact rates for the Oort cloud and Neptune families of micrometeoroids are shown in Fig. 3.

A higher-speed population of micrometeoroids, whose velocities indicate an origin outside of the Solar System (Taylor et al., 1996), has low flux compared to the asteroidal and cometary populations and was not considered in our study.

Assumptions that were used for estimating the effects of gravitational focusing of meteoroids and variations of their number flux distribution with position in the Solar System have an estimated factor of ~ 10 uncertainty in our results (Moses, 1992). The total mass flux intercepted by Triton from the combined mass flux distribution is approximately 5 kg s^{-1}, assuming an impact area of πR_T^2.

Due to the addition of Neptune's and Triton's orbital velocities, the velocity of an incoming meteoroid relative to Triton can be sufficient to strip electrons off the ablated material via impact ionization with Triton's atmosphere. The ionization of the atmospheric gases will be less important on Triton due to the smaller typical velocity. For the average terrestrial meteoroid (with incoming speed ~ 20 km s^{-1}) this

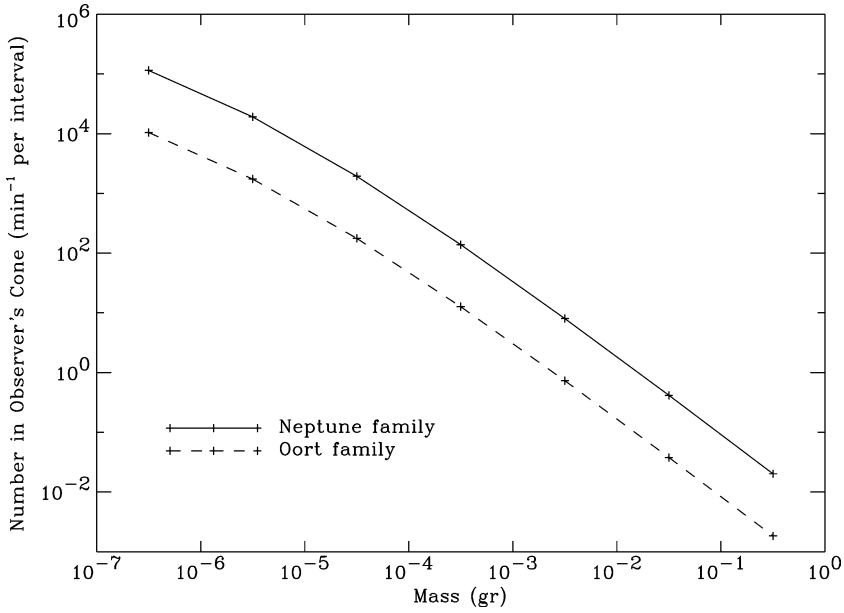

Fig. 3. Estimated impact rate of micrometeoroids onto Triton's atmosphere. The two mass flux distributions defined by Moses (1992) were extended to higher masses and converted to a number flux. That flux was then multiplied by 60, to convert to a count per minute, and by $\pi(30 \times 10^5)^2$, the effective area of a surface-based detector with an opening angle whose half width is 45° and an ablation altitude of 30 km.

impact ionization process is the source of the meteor trails that are detected by both optical detectors and radar. At Triton, the modulation of the impact velocity with changes in the orbital phase of Triton about Neptune will cause meteors to be more visible when Triton is moving in the prograde heliocentric direction (between Neptune and the Sun).

The impact speeds (v_I) of meteoroids on Triton depend on the heliocentric velocity of the meteoroid far from Neptune ($\vec{v}_m$), the heliocentric velocity of the Neptune–Triton system ($|\vec{v}_p| = 5.5$ km s^{-1}), the angle (θ) between $\vec{v}_p$ and $\vec{v}_m$, the orbital velocity of Triton around Neptune ($|\vec{v}_s| =$ 4.4 km s^{-1}), and the phase of Triton's orbit (ϕ, measured from the point where Triton crosses Neptune's orbit outbound). All velocities are assumed to be in the orbital plane of Neptune and values are from Tholen et al. (2000). The magnitude of v_I is

$$v_I^2 = v_{T,g}^2 + v_{N,g}^2 + \left|\vec{v}_m - (\vec{v}_p + \vec{v}_s)\right|^2 \quad (1)$$

$$= v_{T,g}^2 + v_{N,g}^2 + v_m^2 - 2v_m v_p \cos\theta + v_p^2 + v_s^2 + 2v_s\left[v_p \sin\phi - v_m \sin(\phi + \theta)\right], \quad (2)$$

where $v_{T,g} = 1.45$ km s^{-1}, the escape velocity of Triton and $v_{N,g} = 6.34$ km s^{-1}, the velocity required to escape from Neptune's gravity at Triton's orbit. Figure 4 illustrates the various quantities and their relationships.

The magnitude of v_m ranges from 7.74 km s^{-1}, the perihelion velocity of a parabolic, heliocentric orbit with a perihelion at 30 AU (the Oort cloud particles of Moses (1992)) to 2.97 km s^{-1}, the aphelion velocity of an elliptic, heliocentric orbit with a perihelion at 5.2 AU (the orbit of Jupiter) and an aphelion at 30 AU (the Neptune family of Moses (1992)). Figure 5 shows v_I as a function of θ for $|\vec{v}_m| = 5.47$ km s^{-1}, corresponding to the orbital speed of a micrometeoroid in a circular orbit at 30 AU, striking Triton at an angle θ.

For the maximum speed of a meteoroid of $|\vec{v}_m| =$ 7.74 km s^{-1} the relative impact velocity reaches almost 19 km s^{-1} while even for the lower limit $|\vec{v}_m| = 2.97$, $v_I > 10$ km s^{-1} (sufficient for ablation) for at least some orbital phases and values of θ. We will use $v_I = 10$ and 15 km s^{-1} as examples.

The composition of the incoming meteoroids can range from icy to stony to metallic. Iron meteoroids are rare in the Solar System and were not considered. At 1 AU the stony chondrites are the most common. At 30 AU icy particles may be the most common. We will consider the brightness of both stony and water ice micrometeoroids entering the atmosphere of Triton with values of v_I derived above. A summary of typical physical properties of the stony and icy meteoroids is in Table 1. These values are adapted from Moses (1992) and represent the limits of meteor visibility in Triton's atmosphere.

4. Physics of meteors at Triton

A meteoroid ramming into a dense atmosphere heats as the kinetic energy of impacting atmospheric gas is converted into internal energy. This produces melting and evaporation of surface material (Öpik, 1958). Impacts of atmospheric gases can also sputter material off of the particle. The net process of losing surface material is called ablation.

The equations describing the acceleration, heating, and mass loss of a micrometeoroid along its path through any atmosphere are well established. The form of those equations used in this study are discussed by Pesnell and Gre-

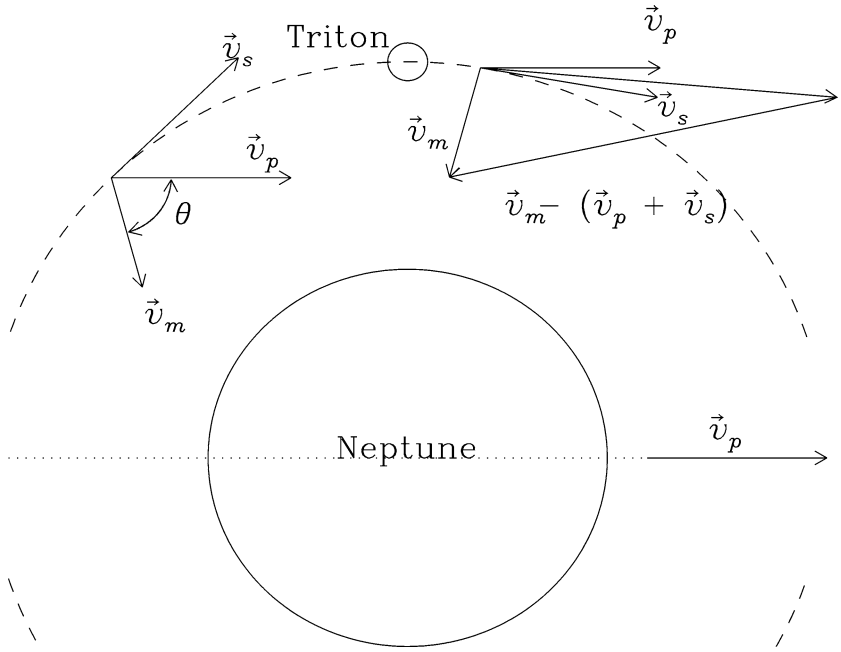

Fig. 4. A schematic showing the definition of velocities in the Neptune–Triton system and the angle of impact (θ) used to calculate the impact speed at Triton (v_I in Eq. (2)). Neptune and Triton are shown as circles, the orbit of Triton around Neptune as a dashed line and the orbit of the Neptune–Triton system around the Sun as a dotted line (not to scale). The left set of vectors show that θ is the angle between $\vec{v}_m$ and $\vec{v}_p$. The right set of vectors shows an example that gives the relative impact velocity of meteoroids toward Triton before they are influenced by the gravitational acceleration of either Triton or Neptune. The thin line is an intermediate construction.

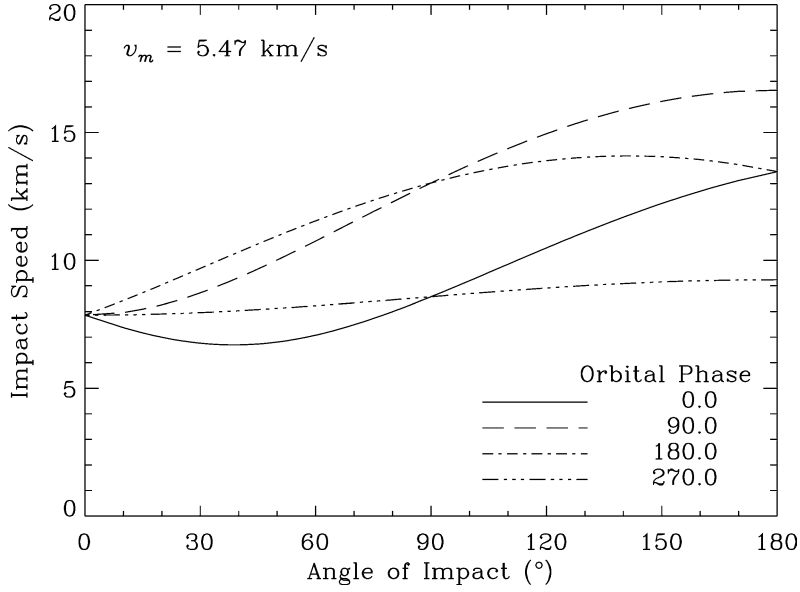

Fig. 5. The variation of relative impact speed with angle of impact (θ) and orbital phase of Triton (ϕ) for $v_m = 5.47$ km s^{-1}, the orbital speed of a circular orbit at 30 AU. Four values of ϕ (in °) are listed in the legend box while θ is treated as a continuous variable.

Table 1
Material properties of meteoroids

Material	log P_v (dyne cm^{-2})	Q_{evap} (ergs gr^{-1})	μ	ρ_m (gr cm^{-3})	ε	c_V (ergs gr^{-1} K^{-1})
Rock	$13.176 - 24605/T$	7.4×10^{10}	50	3.4	0.8	9.6×10^{6}
Ice	$11.5901 - 2104.2/T$	2.65×10^{10}	19	1.2	0.9	4.2×10^{7}

Values adapted from Moses (1992). Symbols represent the vapor pressure (P_v), heat of evaporation (Q_{evap}), mean molecular mass (μ, in amu), mass density (ρ_m), emissivity (ε), and specific heat (c_V).

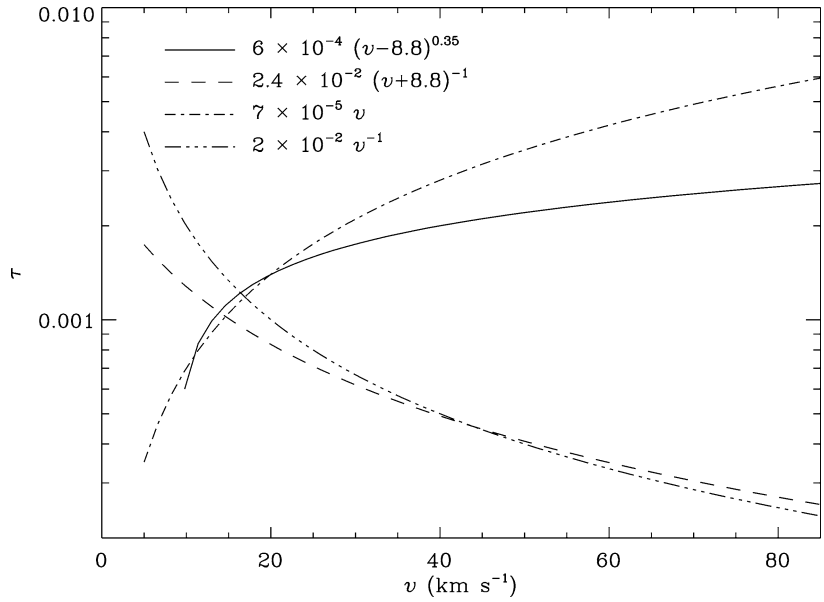

Fig. 6. Several forms of the luminous efficiency used in Eq. (3), shown as a function of the meteoroid velocity. The top two curves in the legend are from Bronshten (1983) and the bottom two curves are from Adolfsson et al. (1996). The curves that increase with velocity are appropriate for stony meteoroids while the curves that decrease with velocity are used with icy cometary material. For meteors in Triton's atmosphere possible values of τ will vary from 0.04 to 0.4%.

bowsky (2000). To study the visibility of meteors, those equations are augmented by an estimate of the intensity of emitted radiation. Emission line spectra of meteors produced by stony micrometeoroids at Triton will be similar to those at Earth as the N_2-dominated atmospheric contributions are nearly the same for both bodies. Roughly 1/2 of the spectral intensity of a meteor due to a stony meteoroid resides in many, low-intensity lines of Fe, Cr, and Ni (summarized in Bronshten (1983); an example of a meteor spectra due to a slow meteor is found in Millman and Cook (1959)). The Ca II H and K lines at 3698 and 3934 Å can be the brightest spectral features. Other strong lines include the Na I doublet at 5890/5896 Å and the Mg I triplet at 5184/5173/5167 Å. The transmitivity of the N_2-dominated atmosphere of Triton should be similar to that of the terrestrial atmosphere.

Water-ice meteoroids will have emission spectra consisting of N_2 lines from the atmosphere and lines of hydrogen and oxygen. Unlike the terrestrial case, where the O and O_2 lines are dominated by atmospheric emissions, spectra at Triton would contain only the meteoric O and O_2 components. Indeed, one major effect of meteoric input could be the deposition of oxygen-rich material into the atmosphere of Triton, similar to the atmospheres of the gas giants (Moses et al., 2000).

The intensity of radiation seen by a scotopic (or dark-adapted) eye is approximated by applying the *S* filter described by Öpik (1958). The fraction of the lost meteoroid kinetic energy that is radiated in the spectral range of the *S* filter is

$$I_S = -\frac{\tau_S}{2} v^2 \frac{dm}{dt} \text{ ergs s}^{-1}, \tag{3}$$

where v is the instantaneous velocity and τ_S is the luminous efficiency. Forms of τ_S for several meteoroid compositions are shown as a function of v in Fig. 6.

Typical values of τ_S are near 10^{-3}, independent of the composition of the meteoroid, for the relative impact velocities of visible meteors at Triton. Using the relationship from Öpik (1958, Eq. (8.21)), I_S is converted to the absolute scotopic magnitude of a source at a distance of 100 km (M_S), corrected for the use of a different detector, and then to an apparent magnitude at the surface of Triton:

$$m_{\text{app}} = \overbrace{24.3 - 2.5 \log I_S}^{M_S} + \underbrace{M_{\text{cc}}}_{\text{color}} + \overbrace{5 \log z/100}^{\text{distance}}. \tag{4}$$

The color correction M_{cc} transforms M_S into a photographic magnitude and was estimated to be $M_{\text{cc}} = -1\overset{\text{m}}{.}8$ by Jacchia (1957). A bare CCD covers a larger wavelength interval than either the *S* filter or photographic emulsions (see Fig. 3.2 in Howell (2000)) so M_{cc} may be underestimated for an unfiltered CCD used as a meteor detector. Meteors with $m_{\text{app}} > 7.5$ will be visible to a ground-based observatory on Triton. The accuracy of M_S was estimated as $0\overset{\text{m}}{.}5$ by Öpik (1958) and we use this as an estimate of the uncertainty in m_{app}.

5. The visibility of meteors at Triton

Trajectories of spherical particles with masses between 10^{-11} and 10 g were integrated through the Triton atmosphere to obtain ablative mass loss curves for each assumed meteoroid composition and velocity. Those curves

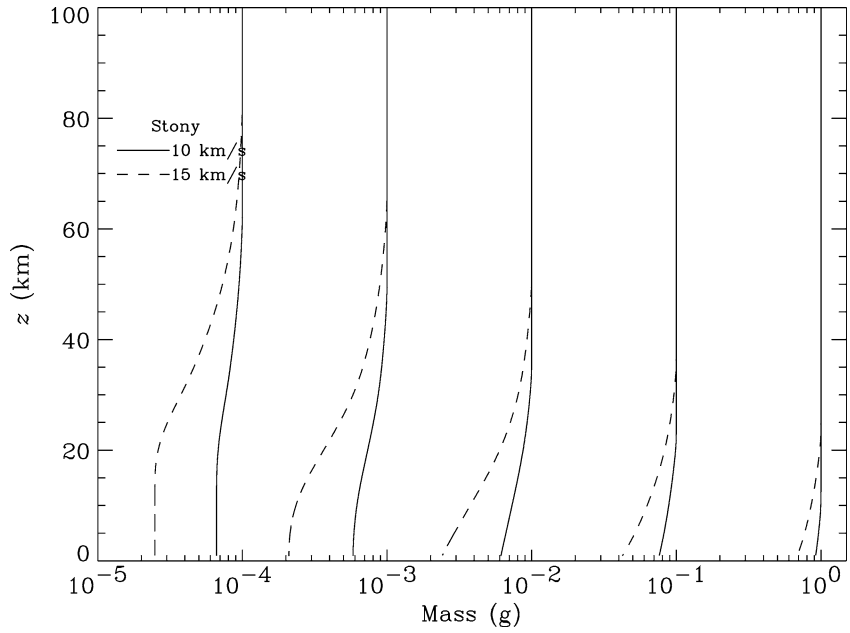

Fig. 7. Calculated variation of mass for stony meteoroids entering Triton's atmosphere at 10 (solid) and 15 km s^{-1} (dashed). The initial masses can be read off of the top axis.

were then used to estimate the brightness profiles for meteors at Triton using Eqs. (3) and (4). Trajectories were started at an initial altitude of 400 km with an angle of incidence of 45°. The calculations were stopped when the altitude of the meteoroid reached an altitude of 1 km. Initial speeds chosen were 10 and 15 km s^{-1}, representative of entry speeds into Triton's atmosphere. The adaptive stepsize Runge–Kutta algorithm described by Pesnell and Grebowsky (2000) was used to integrate the ablation equations in time along the meteoroid's trajectory, ensuring that the rapid acceleration region will be accurately resolved. Due to the low velocities of the incoming particles, sputtering contributes little to the ablation process. Fragmentation of the micrometeoroids was not considered as the particle masses were deemed too small to break up when subjected to the dynamic pressure of entry. The properties used for the stony and icy meteoroids are listed in Table 1.

The variation of the mass of the meteoroids was calculated as a function of altitude for masses in the range 10^{-4}–1 g. Although masses less than 10^{-2} g do not produce meteors visible at the surface of Triton, information from smaller masses is useful when interpreting the results of the calculations. Masses above 1 g also create visible meteors but they only strike Triton at most once every 5–10 hours.

Mass variations for stony meteoroids are shown in Fig. 7 for initial velocities of 10 and 15 km s^{-1} and 5 initial masses logarithmically spaced between 10^{-4} and 1 g. The smallest mass (10^{-4} g) ablates to almost the value predicted by the analytic meteor equation (Eq. (27) in Hughes (1978)) as can be seen in Table 2.

Remnant fractions are predicted by the meteor equation by assuming a balance between frictional heating and evaporative cooling. By including radiative cooling in our numerical calculations, the remnant fraction in the stony meteors has increased above those in the meteor equation. Icy particles have a lower heat of evaporation ($Q_{\rm evap}$) and ablate more completely than stony particles (see Fig. 8).

Table 2
Remnant fractions of meteoroids at Triton

Mass (g)	Stony		Icy	
	10 km s^{-1}	15 km s^{-1}	10 km s^{-1}	15 km s^{-1}
10^{-4}	0.66	0.25	9.6×10^{-2}	5.1×10^{-3}
10^{-3}	0.58	0.21	9.7×10^{-2}	5.1×10^{-3}
10^{-2}	0.61	0.24	0.10	5.1×10^{-3}
0.1	0.76	0.42	0.14	5.6×10^{-3}
1.0	0.92	0.71	0.32	3.1×10^{-2}
M.E.	0.43	0.15	9.5×10^{-2}	5.0×10^{-3}

M.E. is the remnant fraction using the meteor equation in Hughes (1978) and does not depend on the initial mass of the bolide.

Therefore, as the brightness of a meteor is directly related to the mass loss rate (see Eq. (3)), icy meteoroids will create brighter meteors. The approximate altitude of the brightest meteor is where the rate of decrease in the mass is greatest. Figure 8 shows that icy micrometeoroids with $m \sim 10^{-2}$ g will create meteors between altitudes of 20 to 40 km. For anticipated meteoroid fluxes in the outer Solar System, micrometeoroids near this mass will be the largest source of visible meteors. Hence, the altitude of 30 km is the estimated average location for meteor-producing ablation. Stony micrometeoroids also have meteor-producing mass loss in that altitude region (see Fig. 7).

Figure 9 shows the brightness of meteors from water ice micrometeoroids initially moving at 10 and 15 km s^{-1}. For both values of the initial velocity, meteoroids with mass > 0.1 g will make it to the surface while still ablating (see

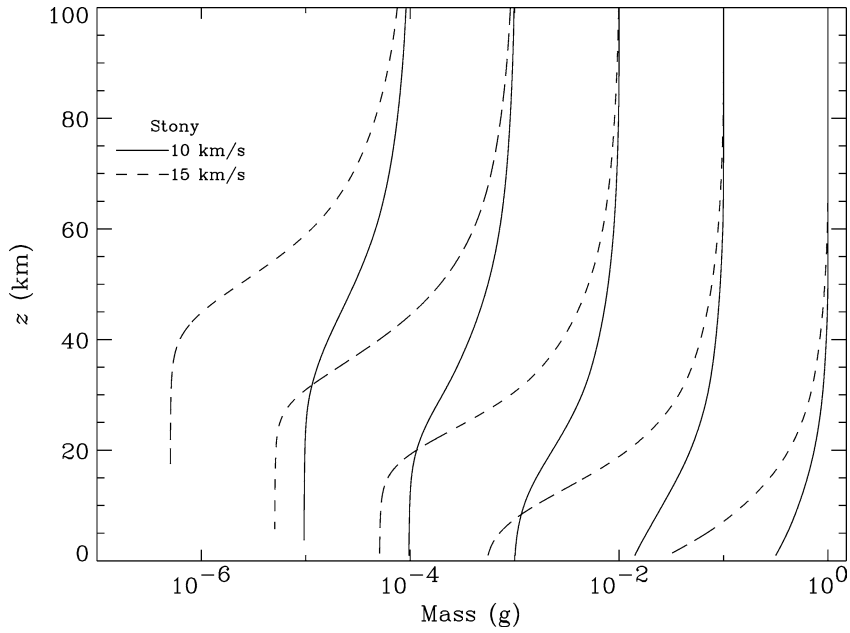

Fig. 8. Calculated variation of mass for ice meteoroids entering Triton's atmosphere at 10 (solid) and 15 km s^{-1} (dashed). The initial masses can be read off of the top axis.

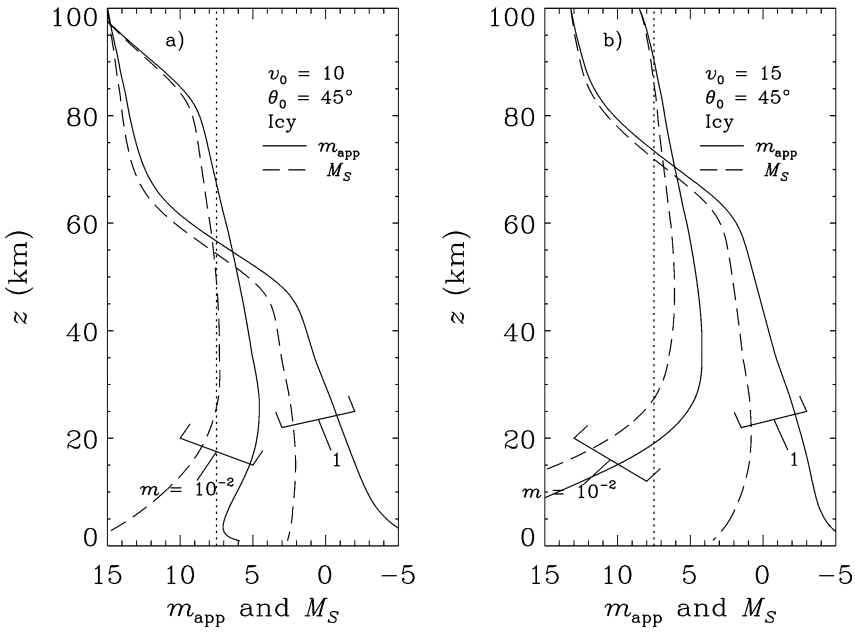

Fig. 9. Calculated brightness of icy meteoroids entering Triton's atmosphere at 10 (a) and 15 km s^{-1} (b). Both panels show $m_{\rm app}$, the apparent magnitude at the surface, and M_S, the "absolute" magnitude of a meteor at a distance of 100 km, as solid and dashed lines, respectively.

Fig. 8). This would result in those meteors being visible at the surface. Figure 9 shows that these near-surface meteors have very long lengths. This would allow surface observations of the entire trail to easily resolve the time dependence of the chemistry and diffusion processes. In particular, ultraviolet radiation emitted by the meteor that cannot be seen from surface meteor observations at Earth would be observable at Triton.

Comparing the luminosity effects of meteoroids with $m = 10^{-2}$ g at different phases of Triton's orbit around Neptune ($\vec{v}_s$) would show the dependence of the drag force on the initial velocity. For $v_I = 15$ km s^{-1}, the $m = 10^{-2}$ g meteoroid shows only a modest enhancement in $m_{\rm app}$ over M_S. The evaporation of this meteoroid occurs above an altitude of 20 km. By contrast, the same mass with $v_I =$ 10 km s^{-1} starts to ablate 10–20 km lower in altitude and continues to ablate until the surface. When viewed from the surface, the brightness of the slower meteoroid actually has a minimum at an altitude of 5 km where the proximity to the surface overcomes the decrease in ablative

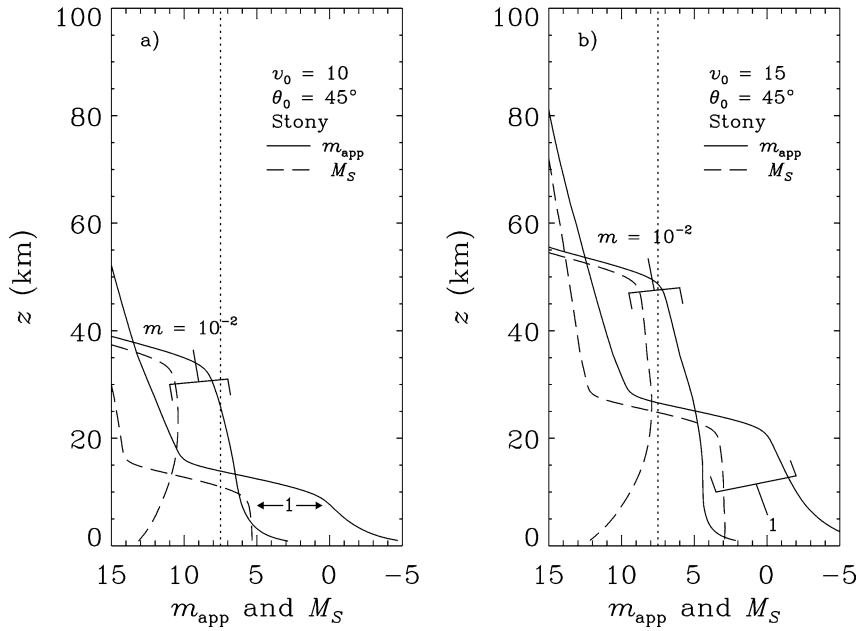

Fig. 10. Calculated brightness of stony meteoroids entering Triton's atmosphere at 10 (a) and 15 km s^{-1} (b). Both panels show m_{app} and M_S as solid and dashed lines, respectively.

mass loss (and meteor intensity) with time along the trajectory.

In contrast, a 1 g icy meteoroid continues to ablate to the surface and has a roughly 10 magnitude enhancement in its brightness as it nears the surface (Figs. 9a, 9b). Even though slower meteoroids with this mass ablate at a lower altitude (higher column density), meteors with both initial velocities, as seen in Figs. 9a, 9b, exhibit large enhancements in brightness due to their proximity to the surface.

The brightness of stony meteoroids (chondrites) as they pass through Triton's atmosphere are shown in Fig. 10. As with the icy meteoroids in Fig. 9, meteoroids with $m > 10^{-1}$ g strike the surface while still ablating. Meteoroids with $m \geqslant 10^{-2}$ g will produce visible meteors all the way to the surface, although those with $m = 10^{-2}$ g would be marginally visible without the proximity effect.

6. Further implications

In addition to visible meteors, there are other anticipated effects that incoming meteoroids have on the atmosphere of Triton. For example, layers of metallic ions and molecules may be persistent features of Triton's atmosphere. Metallic ions, such as Na^+, Mg^+, Ca^+, and Fe^+ would be created both during the ablation process and by ionization of the deposited neutral material while it is diffusing through the atmosphere. Solar ultraviolet radiation that is not absorbed by the N_2-dominated atmosphere of Triton is one source of ionization. Each metallic ion species would be produced at a different altitude in the atmosphere as the optical depth for the ionizing radiation varies from species to species (as illustrated for the terrestrial atmosphere by Swider (1969)). This is in contrast to the metallic ions in the Earth's atmosphere, which are generated by charge-exchange with ambient ionospheric species and are closely spaced in altitude, but it is similar to the martian atmosphere (Pesnell and Grebowsky, 2000). Charge exchange can also ionize the ablated metallic atoms in Triton's ionosphere if the metal atoms exist in a region with a substantial concentration of ambient ions. Cosmic rays penetrate to the surface of Triton and will ionize many of the gas species (including the metallic species) in the lower reaches of the atmosphere.

Mixed with and extending below the metallic ion layer could be a neutral atomic layer, and below that, molecular metallic compounds. The detailed chemistry of the conversion from atomic to molecular compounds is dependent on reactions with somewhat uncertain rates (especially at the exceedingly low temperatures of Triton's atmosphere), but the topside of the metal atom ion layer is itself controlled by fairly simple chemistry not affected by these uncertainties (Pesnell and Grebowsky, 2000). Condensation of ablated atoms and molecules into dust as well as attachment of metallic ions onto dust would also have atmospheric consequences. In the terrestrial atmosphere these processes could be seeds of cloud formation, such as noctilucent clouds (Hunten et al., 1980). Hence, if ablated material could form ions and charged particles near Triton's surface they could serve as nucleation centers to generate the haze layers observed in the atmosphere (Yelle et al., 1995). Finally, most metallic molecular compounds would be transported downward and form condensates on the surface of Triton. These aspects are currently being modeled.

7. Conclusions

We have modeled the brightness of meteors in Triton's atmosphere as observed from the surface of the satellite. Meteors would be readily visible from the surface whether they were composed of water ice or rock. Meteoroid masses greater than 10^{-2} g would form visible meteors, particularly when Triton's orbit around Neptune carries it between Neptune and the Sun. At this orbital phase the orbital motions of Triton around Neptune and Neptune/Triton around the Sun combine to yield maximum meteoroid impact velocities of almost 19 km s^{-1}.

The presence of meteors is just one aspect of the significance of meteoroids in the thin atmosphere of Triton. Introducing meteoric material into the atmosphere of gas giant planets has been predicted to have profound implications for the chemistry within those atmospheres (Moses, 1992; Moses and Bass, 2000; Moses et al., 2000). In particular, the oxygen and carbon atoms present in large quantities in both stony and icy micrometeoroids would be ablated into the atmosphere to form H_2O, CO, and CO_2. The thermal structure of Triton's atmosphere is formed by a balance between the energy inputs (solar EUV radiation and energetic particles from Neptune's magnetosphere) and emission in a CO rotational band (Müller-Wodarg, 2002). Introducing O from meteoric material (and possibly C) could act to cool Triton's atmosphere. Whether the amount of oxygen injected into these atmospheres is sufficient to generate the observed amounts of those molecules is an active research question (Grebowsky et al., 2002) whose answer depends on the actual amount of injected material. Although not on any current planned mission, surface-based measurements of the ablating particles in Triton's atmosphere could provide direct observations of this input.

Acknowledgment

This work was supported, in part, by contract NAS5-00142 through the Goddard Space Flight Center.

References

Adolfsson, L.G., Gustafson, B.Å.S., Murray, C.D., 1996. Mars' atmosphere as a meteoroid detector. Icarus 119, 144–152.

Bronshten, V.A., 1983. Physics of Meteoric Phenomena. Reidel, Dordrecht.

Broadfoot, A.L., 21 colleagues, 1989. Ultraviolet spectrometer observations of Neptune and Triton. Science 246, 1459–1466.

Grebowsky, J.M., Moses, J.I., Pesnell, W.D., 2002. Meteoric material—an important component of planetary atmospheres. In: Mendillo, M., Nagy, A., Waite, J.H. (Eds.), Atmospheres in the Solar System: Comparative Aeronomy. In: Geophysical Monograph, vol. 130. American Geophysical Union, Washington, DC, pp. 235–244.

Grün, E., Zook, H.A., Fechtig, H., Giese, R.H., 1985. Collisional balance of the meteoritic complex. Icarus 62, 244–272.

Grün, E., Gustafson, B.Å.S., Dermott, S.F., Fechtig, H., 2001. Interplanetary Dust. Springer-Verlag, New York.

Hedin, A.E., 1983. Global empirical model of the Venus thermosphere. J. Geophys. Res. 88, 73–83.

Hedin, A.E., 1987. MSIS-86 thermospheric model. J. Geophys. Res. 92, 4649–4662.

Howell, S.B., 2000. Handbook of CCD Astronomy. Cambridge Univ. Press, New York.

Hughes, D.W., 1978. Meteors. In: McDonnell, J.A.M. (Ed.), Cosmic Dust. Wiley–Interscience, New York, pp. 123–184.

Hunten, D.M., Turco, R.P., Toon, O.B., 1980. Smoke and dust particles of meteoric origin in the mesosphere and stratosphere. J. Atmos. Sci. 37, 1342–1357.

Ip, W.-H., 1990a. Meteoroid ablation processes on Titan. Nature 345, 511–512.

Ip, W.-H., 1990b. On the ionosphere of Triton: an evaluation of the magnetospheric electron precipitation and photoionization effect. Geophys. Res. Lett. 17, 1713–1716.

Jacchia, L.G., 1957. On the "color index" of meteors. Astron. J. 62, 358–361.

Kim, Y., Fox, J.L., Grebowsky, J.M., Pesnell, W.D., 2001. Meteoric ions in the ionosphere of Jupiter. Icarus 150, 261–278.

Krasnopolsky, V.A., Cruikshank, D.P., 1995. Photochemistry of Triton's atmosphere and ionosphere. J. Geophys. Res. 100, 21271–21286.

Lyons, J.R., Yung, Y.L., Allen, M., 1992. Solar control of the upper atmosphere of Triton. Science 256, 204–206.

Millman, P.M., Cook, A.F., 1959. Photometric analysis of a spectrogram of a very slow meteor. Astrophys. J. 130, 648–662.

Molina-Cuberos, G.J., Lammer, H., Stumptner, W., Schwingenschuh, K., Rucker, H.O., López-Moreno, J.J., Rodrigo, R., Takano, T., 2001. Ionospheric layer induced by meteoric ionization in Titan's atmosphere. Planet. Space Sci. 49, 143–153.

Moses, J.I., 1992. Meteoroid ablation in Neptune's atmosphere. Icarus 99, 368–383.

Moses, J.I., Bass, S.F., 2000. The effects of external material on the chemistry and structure of Saturn's ionosphere. J. Geophys. Res. 105, 7013–7052.

Moses, J.I., Lellouch, E., Bézard, B., Gladstone, G.R., Feuchtgruber, H., Allen, M., 2000. Photochemistry of Saturn's atmosphere. II. Effects of an influx of external oxygen. Icarus 145, 166–202.

Müller-Wodarg, I.C.F., 2002. The application of general circulation models to the atmospheres of terrestrial-type moons of the giant planets. In: Mendillo, M., Nagy, A., Waite, J.H. (Eds.), Atmospheres in the Solar System: Comparative Aeronomy. In: Geophysical Monograph, vol. 130. American Geophysical Union, Washington, DC, pp. 307–318.

Murad, E., Williams, I.P. (Eds.), 2002. Meteors in the Earth's Atmosphere. Cambridge Univ. Press, Cambridge.

Öpik, E.J., 1958. Physics of Meteor Flight in the Atmosphere. Interscience, New York.

Pesnell, W.D., Grebowsky, J.M., 2000. Meteoric magnesium ion layers in the martian atmosphere. J. Geophys. Res. 105, 1695–1707.

Strobel, D.F., Summers, D.E., 1995. Triton's upper atmosphere and ionosphere. In: Cruikshank, D.P. (Ed.), Neptune and Triton. Univ. of Arizona Press, Tucson, pp. 1107–1148.

Swider Jr., W., 1969. Processes for meteoric elements in the E-region. Planet. Space Sci. 17, 1233–1246.

Taylor, A.D., Baggaley, W.J., Steel, D.I., 1996. Discovery of interstellar dust entering the Earth's atmosphere. Nature 380, 323–325.

Tholen, D.J., Victor, V.G., Cox, A.N., 2000. Planets and satellites. In: Cox, A.N. (Ed.), Allen's Astrophysical Quantities, fourth ed. Springer-Verlag, New York, pp. 293–313.

Tyler, G.L., 9 colleagues, 1989. Voyager radio science observations of Neptune and Triton. Science 246, 1466–1473.

Yelle, R.V., Lunine, J.I., Pollack, J.B., Brown, R.H., 1995. Lower atmospheric structure and surface–atmosphere interactions on Triton. In: Cruikshank, D.P. (Ed.), Neptune and Triton. Univ. of Arizona Press, Tucson, pp. 1031–1105.